J Physiol Sci (2011) 61:151–160
DOI 10.1007/s12576-011-0132-4

ORIGINAL PAPER

The relationship between aortic baroreceptor activity and arterial pressure is not monotonic

Chris P. Bolter · Michael J. Turner · Carolyn J. Barrett

Received: 1 November 2010 / Accepted: 3 January 2011 / Published online: 15 January 2011

Abstract Previous reports indicate that when aortic pressure (AP) falls below the threshold (P_{th}) for baroreceptor sensitivity, activity in the aortic depressor nerve (ADN) may increase. To quantify and explain this anomalous behaviour, we analysed curves describing the relationship of baroreceptor fibre activity in rabbit left ADN to AP. Data were obtained in anaesthetised New Zealand White rabbits. Occlusion and release of cuffs around the inferior vena cava and descending aorta generated AP ramps (25–140 mmHg). Response curves were obtained for 173 fibres in 26 animals. Thirty percent of curves had a nadir (J-shaped curve), and in 40% activity was always present. In fibres showing activity below P_{th}, firing was predominantly diastolic, switching to systolic firing at P_{th}. The unusual behaviour of a substantial fraction of aortic baroreceptors below P_{th} accounts for the J-shaped response curve of the whole ADN. We suggest that fibres that fire during diastole at pressures below P_{th} may have sensory endings close to the origin of the left subclavian artery. As a consequence of this anatomical location, low pressures can impose strain on these receptors, which is then relieved by the systolic pulse.

Keywords Baroreceptor · Baroreflex · Aortic arch

C. P. Bolter (✉) · M. J. Turner
Department of Physiology, School of Medical Sciences, University of Otago, PO Box 913, Dunedin 9054, New Zealand
e-mail: chris.bolter@otago.ac.nz

C. J. Barrett
Department of Physiology, University of Auckland, Auckland, New Zealand

Introduction

The arterial baroreceptors and their associated afferent fibres provide the sensory arm of the first order baroreflex control of arterial pressure. Stress and strain in the wall of the artery are determined by the arterial pressure, and it is these variables that are monitored by the baroreceptors. Circumferential distortion of the vessel, which occurs at lower and mid-range arterial pressures, is reported primarily by baroreceptors coupled to myelinated afferent fibres (A-fibre baroreceptors) [1–7]. Baroreceptors coupled to unmyelinated afferent fibres (C-fibre baroreceptors) appear to respond primarily to compression of the arterial wall [8] and report arterial pressure in the middle and higher range of pressure [9–12]. In combination, signals from A- and C-fibre baroreceptors will relay information about the wide range of daily arterial pressures to central nervous structures.

One might expect that the mechanical distortion of the arterial wall responsible for the activation of both A- and C-fibre baroreceptors would increase progressively as arterial pressure increases, and thus result in a monotonic relationship (response curve) between baroreceptor activity and mean arterial pressure (MAP). However, we have reported that the relationship between multifibre activity in the rabbit aortic depressor nerve (ADN) and MAP is not monotonic but assumes a 'J-shape' (Fig. 1 in [13]). Baroreceptor activity was monitored during slow ramps of MAP extending from 25 to 140 mmHg. There was always activity at the lowest pressure, and activity decreased as pressure was raised until a threshold pressure (P_{th}) was reached; above P_{th}, activity increased monotonically. As far as we aware there has been no other report that the baroreceptor response curve from the intact ADN assumes this shape. We have also recorded activity from single

fibres, and some of these possessed J-shaped response curves with a nadir at P_{th} [13]. Thus the J-shaped multifibre response curve may be attributable, at least in part, to the behaviour of a substantial subpopulation of aortic baroreceptors within the ADN [13]. Indeed, there are limited reports of fibres possessing these appropriate firing characteristics [2, 3, 11].

In an attempt to explain the basis of the J-shaped response curves seen in multifibre preparations of the ADN we have re-analysed data obtained in two sets of experiments, termed series 1 and series 2. Series 1 data were obtained ~10 years prior to series 2. Using series 1 data, we re-examined the response curves of a large set of individual baroreceptor fibres, describing and quantifying their behaviour at lower pressures. Based on the presence or absence of silence and/or a nadir at lower pressures, we identified and quantified four different types of response curve. Using series 2 data, we investigated the basis of the frequent anomalous behaviour of baroreceptors at lower pressures. We measured pressure in the aortic arch using a catheter tip manometer. In some instances we obtained simultaneous recordings of aortic diameter. Collectively, these measurements allowed us to propose an explanation for the non-monotonic, J-shaped response curve of a substantial population of aortic baroreceptors.

Methods

Ethics approval

The experimental procedures were approved by the Committee on Ethics in the Care and Use of Laboratory Animals, University of Otago.

Animals

Both series of experiments were performed using adult New Zealand White rabbits of either sex (2.2–5.0 kg).

Preparations

Series 1 Animals were anaesthetised with 30–40 mg kg^{-1} sodium pentobarbitone i.v. in an ear vein. Further anaesthetic was administered as required. Mechanical ventilation was applied through a tracheal cannula, and colonic temperature was maintained at 37–38°C. A short catheter was advanced to the aortic arch through the left brachial artery, and aortic pressure (AP) was measured with a Statham P23DC pressure transducer (Hato Rey, Puerto Rico).

Series 2 Animals were anaesthetised with chloralose (50 mg kg^{-1} i.v.) and urethane (1 g kg^{-1}), with further anaesthetic administered as required. Animals were maintained as described for series 1. A 3F catheter-tip manometer (SPR-249, Millar Instruments, Houston, TX, USA) was inserted into the right femoral artery and advanced to the aortic arch. In some preparations, ultrasonic crystals (5 MHz, 2-mm diameter; Triton Technology, San Diego, CA, USA) were placed on the descending thoracic aorta 4–5 cm caudal to the apex of the aortic arch, and aortic diameter (D_{ao}) was measured using a sonomicrometer (Triton Technology, Model 6).

Generating ramps of systemic arterial pressure

The chest was opened between the fourth and fifth ribs and end-expiratory pressure was set at 3–5 cmH_2O. Perivascular cuffs (5-mm diameter; In Vivo Metric, Healdsburg, CA, USA) were secured around the inferior vena cava and the descending thoracic aorta. Inflation and deflation of the inferior vena cava cuff followed by inflation of the aortic cuff generated pressure ramps that rose from ~25 to ~140 mmHg (at 0.5–1.0 mmHg s^{-1} in series 1, and ~2 mmHg s^{-1} in series 2).

Recording baroreceptor activity

The left ADN was exposed in the neck and cut at its junction with the superior laryngeal nerve. For recording multifibre activity, the intact ADN was placed on a pair of platinum electrodes and embedded in a fast-curing silicone gel (Wacker SilGel 604, Wacker-Chemie, Munich, Germany). At least 30 min elapsed before data were collected. To record single fibre baroreceptor activity, the ADN was split into small filaments. Individual filaments were placed over one electrode with the indifferent electrode grounded to the surrounding tissue through a fine cotton thread. Filaments were split repeatedly until the signal from a single afferent fibre was discriminable. Signals from nerve preparations were amplified (Model P15D, Grass Instruments, Quincy, MA, USA and DAM80, World Precision Instruments, Sarasota, FL, USA, for series 1 and series 2 data respectively), and filtered (high and low pass filters: 100 Hz and 10 kHz for multifibre preparations, and 100 Hz and 3 kHz for single fibre preparations).

Data acquisition and analysis

Series 1 Analogue signals of nerve activity and AP were digitized (Vetter PCM, Model 3000A, Rebersburg, PA, USA) and stored on videotape. The tape was replayed and signals appropriately treated prior to recording as a Chart file (Chart 3.4, ADInstruments, Castle Hill, NSW, Australia) from which the data were extracted. Action potential frequency was obtained by passing the electroneurogram

through a custom-made discriminator and counter. Action potentials were counted in 0.2-s bins. For multifibre activity the threshold of the discriminator was set just above the noise level recorded after the AP cuff was deflated at the end of a pressure ramp, when nerve activity was briefly absent.

Series 2 Data were recorded and processed using software in Chart v5.5.6 (ADInstruments). The firing frequency of individual action potentials was obtained from the raw baroreceptor signal using the cyclic variable software. Each recording was inspected closely in order to describe the mechanical events associated with the firing of action potentials.

Results

Series 1: multifibre baroreceptor recording

Figure 1a–f shows examples of response curves from six different preparations randomly selected from 30 similar records obtained over a 3-year period. Each panel shows a single unfitted response curve to a pressure ramp. All response curves are non-monotonic, possessing a J-shape with a nadir in the region of 40–55 mmHg. In all examples there is significant nerve activity at low pressures. All 30 preparations had response curves that conformed to this general pattern. A curve that presents the mean of the individual responses is not presented since it would tend to blur the nadir and shape of the response curve at lower pressures.

Series 1: single fibre baroreceptor recording

Recordings were obtained from 173 separate single baroreceptor fibres in 26 animals. Initial examination of response curves from these fibres suggested that they could be described using a minimum of four categories. This allowed responses to be grouped by two distinct characteristics (Fig. 2). The first characteristic concerns the nature of the pressure-activity relationship—either monotonic or non-monotonic (a J-shape showing a nadir). The second characteristic was the absence or presence of silence (a pressure/pressure range over which a fibre did not fire). Every fibre was placed in a category (types A–D) based on these two response characteristics. For every fibre we quantified five variables. These were the threshold pressure (P_{th}) at which activity began to increase with increasing pressure, and the firing rate at this threshold (F_{th}); the pressure (P_{max}) at which activity reached a maximum (F_{max}); and gain (G) as the ratio $(F_{max} - F_{th})/(P_{max} - P_{th})$. Values of these variables for the four different fibre types were compared using ANOVA followed by Fisher's LSD.

Table 1 shows the categorical distribution of fibres and the values of five measured variables. Almost 50% of fibres (type A) had a 'classic' sigmoidal response curve with silence below P_{th}. Over half the total population did not respond in this manner; curves from 30% of the fibres demonstrated a nadir (Fig. 3a; types C and D), and 40% were never silent over the ramp pressure range (Fig. 3a; types B and D). The features possessed by types A–D most likely explain the overall shape of the multifibre response curves (Fig. 1), which have a nadir and show activity at all pressures tested. Fibres of type B (sigmoidal response curve with no silence at P_{th}) had a significantly higher maximum firing rate than the other three fibre types ($P < 0.01$). Type D fibres (nadir in the response curve with no silence at P_{th}) had lower gain than either type A or C ($P < 0.01$). It should be noted that since the pulse characteristics were not controlled, values for P_{th} and P_{max} are

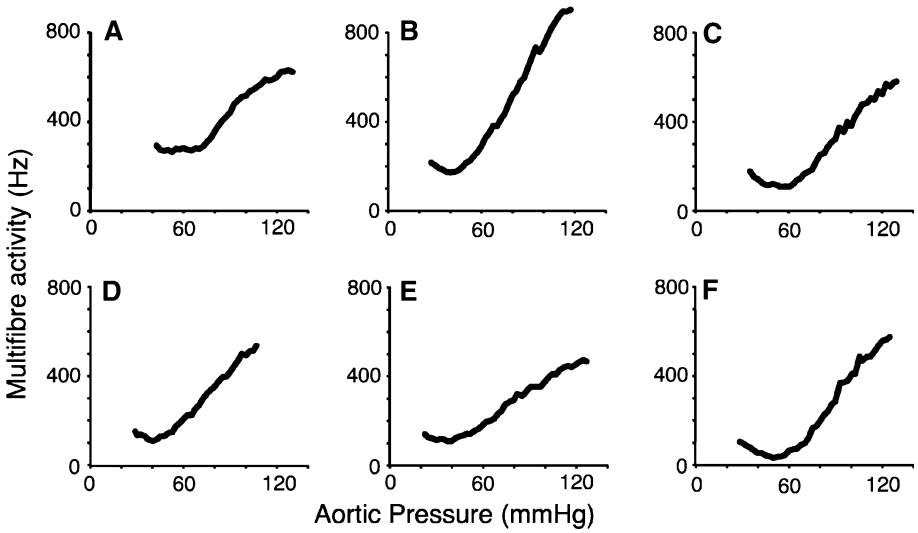

Fig. 1 Examples of response curves obtained in six separate animals showing baroreceptor firing rate in multifibre recordings from the left ADN. All curves possess the two features examined in this paper: significant afferent activity at lower aortic pressures and a J-shape with a distinct nadir. Below the nadir decreasing pressure is associated with increasing firing rate. Similar response curves were obtained from more than 30 individual preparations

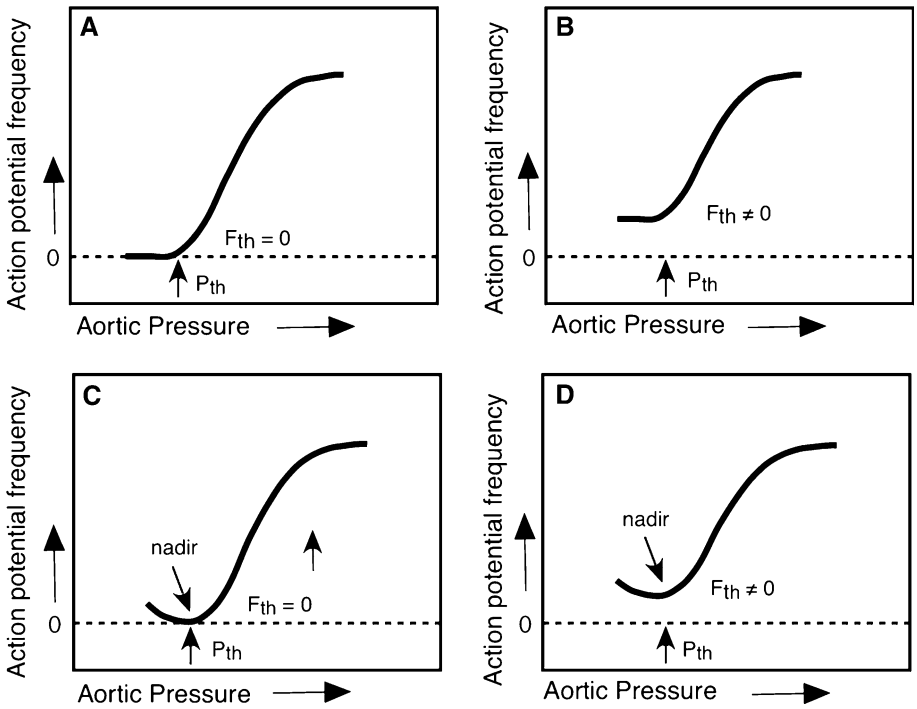

Fig. 2 **a**,**b** Classification scheme for single fibre baroreceptor response curves in the left ADN. Below a threshold pressure (P_{th}), types A and B demonstrate either no activity (**a**) or a constant activity (**b**), and above P_{th}, activity increases with increasing pressure. Types C and D demonstrate a non-monotonic relationship between activity and pressure. Below a nadir, decreasing pressure is associated with an increase in activity. In type C, there is no activity at the nadir, while type D fibres, like type B, are not silent at any pressure ($F_{th} \neq 0$). All four types of fibre reach a maximum firing frequency (F_{max}) at P_{max}

Table 1 Characteristics and population distribution of the four types of baroreceptor fibres classified by their response curves (see Fig. 2)

Type	Number	Percentage	P_{th} (mmHg)	F_{th} (Hz)	P_{max} (mmHg)	F_{max} (Hz)	Gain (Hz/mmHg)
A	83	48	52 ± 10	0	130 ± 13	59 ± 22	0.76 ± 0.28
B	38	22	54 ± 16	13 ± 13‡	135 ± 12	71 ± 21*	0.72 ± 0.29
C	20	12	54 ± 12	0	133 ± 9	60 ± 23	0.76 ± 0.29
D	32	18	56 ± 12	22 ± 16‡,$	132 ± 12	62 ± 17	0.54 ± 0.21**
Never silent (B and D)	70	40					
Display nadir (C and D)	52	30					
Total/mean	173		54 ± 12	7 ± 13	132 ± 12	63 ± 21	0.7 ± 0.3

Primary features of response curves of aortic baroreceptor fibres from the left ADN, grouped (types A, B, C, D; see Fig. 2). Values for fibre characteristics are presented as the mean ± SD

P_{th} Pressure threshold at which activity increases, F_{th} firing rate at P_{th}, P_{max} pressure at which firing rate reaches a maximum, F_{max} maximum firing rate, *gain* mean slope of the response curve between P_{th} and P_{max}

* Significantly different from A; $P < 0.01$

** Significantly different from A, B and C; $P < 0.01$

‡ Significantly different from A and C; $P < 0.01$

$ Significantly different from B; $P < 0.05$

not necessarily comparable with those from other studies. On the other hand, our data do reflect natural responses, and we have assumed that variability in pulse characteristics occurred randomly.

Since the fibres were randomly selected and the sample size was substantial, we considered that the distribution of fibres within the categories, summarised in Table 1, was a reasonable representation of their sampling within a multifibre recording. To see how this multifibre recording might appear, we assembled the responses of the 173 fibres to generate a response curve for a 'multifibre' recording of baroreceptor A-fibres (Fig. 3b). The assembled curve (ALL) possesses the two key features seen in the multifibre response curves in Fig. 1—activity present at all pressures and a nadir at P_{th}.

Series 2: single fibre baroreceptor recording

Using this series of response curves we examined the detailed behaviour of individual baroreceptor fibres during a pressure ramp. The purpose was to examine the relationship between fibre activity and the features of AP in an

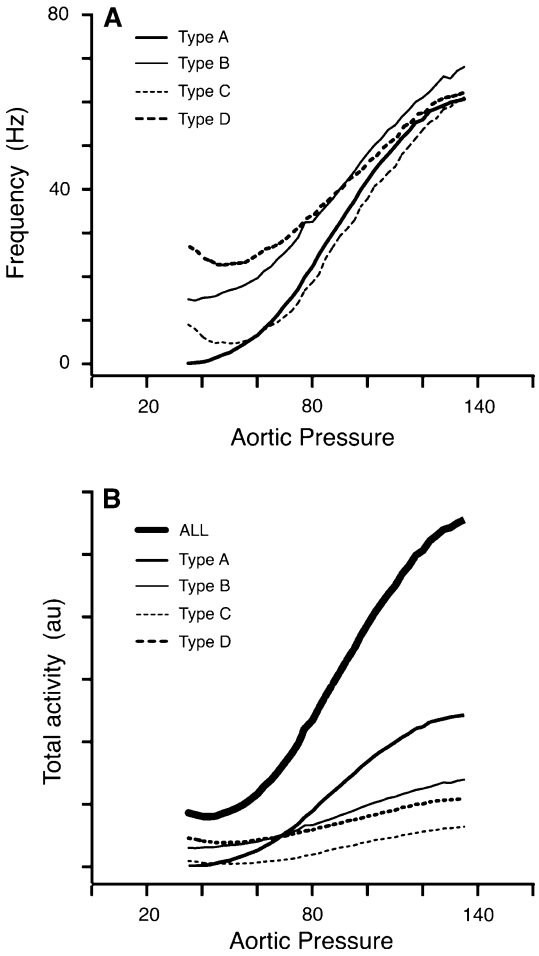

Fig. 3 **a** Mean response curves for the four fibre types defined in Fig. 2. Since the P_{th} for individual fibres differed, the sharp features seen in the response of an individual fibre are smeared in the pooled graphs. However, it is clear that types B and D (40% of total) show substantial firing at all pressures, and that types C and D (30% of total) have a nadir at low pressure, below which firing frequency increases while pressure decreases. **b** An estimate of the relative contribution of each type of baroreceptor to a response curve of a multifibre record from an intact ADN. The curves in this graph were obtained by finding the product of the type mean response curve (**a**) and number of fibres contributing to the type mean. While activity from type A fibres (48%) predominates this multifibre response curve, the contribution of all types of fibres (those never silent and those possessing a low pressure nadir) can be seen clearly in the response labelled *ALL*, which reflects this weighted contribution of the four fibre types

attempt to explain the shape of the response curves and, in particular, the basis of the non-monotonic J-shaped response. Data were obtained from 13 animals. Multifibre recordings of the intact ADN were made prior to nerve splitting. All the multifibre records yielded J-type response curves when activity was measured as either the frequency of individual action potentials (as performed for series 1) or as integrated activity. We obtained recordings from 120 single baroreceptor fibres during pressure ramps, and 44 of these (37%) possessed J-shaped response curves and were designated either type C or D; a similar proportion of series 1 fibres (30%) fell into these two categories (Table 1).

Figure 4a, b shows the ramp responses of one type A and one type B fibre, having monotonic response curves. Both recordings were obtained in the same animal. At the lowest APs, well below P_{th}, the type B fibre was firing at about 50% of F_{max} ($F_{th} \cong 30$ Hz). Firing frequency was relatively constant throughout a cardiac cycle with a small decline coincident with early systole. A small but pronounced increase in systolic firing appeared at P_{th}, which became larger as pressure was raised further. At moderate APs, the pressure pulse produced large fluctuations in aortic diameter (D_{ao}), with a large positive dD_{ao}/dt. At higher APs the aorta was stiffer, and even though pulse pressure was increasing, the pulsatile variations in D_{ao} and dD/dt were much reduced. In all fibre types, reductions in peak positive dD_{ao}/dt and in the amplitude of fluctuations of D_{ao} were associated with an increase in diastolic firing.

A response from a type D fibre is shown in Fig. 5. At the lowest pressures firing was entirely diastolic with up to seven action potentials per cycle, but as the nadir of the response curve was approached, firing rate was reduced to a single action potential during early systole. Above P_{th} the behaviour of this fibre was indistinguishable from types A–C; initially there was an increase in systolic firing, while at higher pressures diastolic firing entered the record. Many type D fibres had a higher discharge rate at the nadir than the example in Fig. 5, such that the mean discharge for type D fibres at P_{th} was 22 ± 16 Hz. There was considerable variation in P_{th} for all fibre types. As an example this is evident in the recording of two type D fibres in Fig. 6, where P_{th} for the fibre with larger amplitude signal occurs $\sim$20 mmHg below the P_{th} for the fibre with the smaller signal. The behaviour of both of these fibres at low pressures matches the description given for the fibre shown in Fig. 6. Indeed, all type C and type D fibres showed similar subthreshold behaviour, with firing at the lowest pressures usually restricted to diastole. The differences between type D and type C fibres were that type C was silent at the nadir and had higher gain (Table 1).

We used ramps of increasing pressure to examine the discharge characteristics of the baroreceptors. It is well established that response curves based on ramps of decreasing pressure demonstrate hysteresis, and a higher value for P_{th} is observed on the descending limb of a ramp. To see whether the direction of pressure change affected the discharge pattern of type C and D fibres, we examined our records for ramps of descending pressure. We had not intended to perform descending ramps, so we searched the records for sections where a steady decline in AP occurred at the time when the cuff around the inferior vena cava was inflated to initiate an ascending ramp. An example of one of these descending ramps and the following ascending

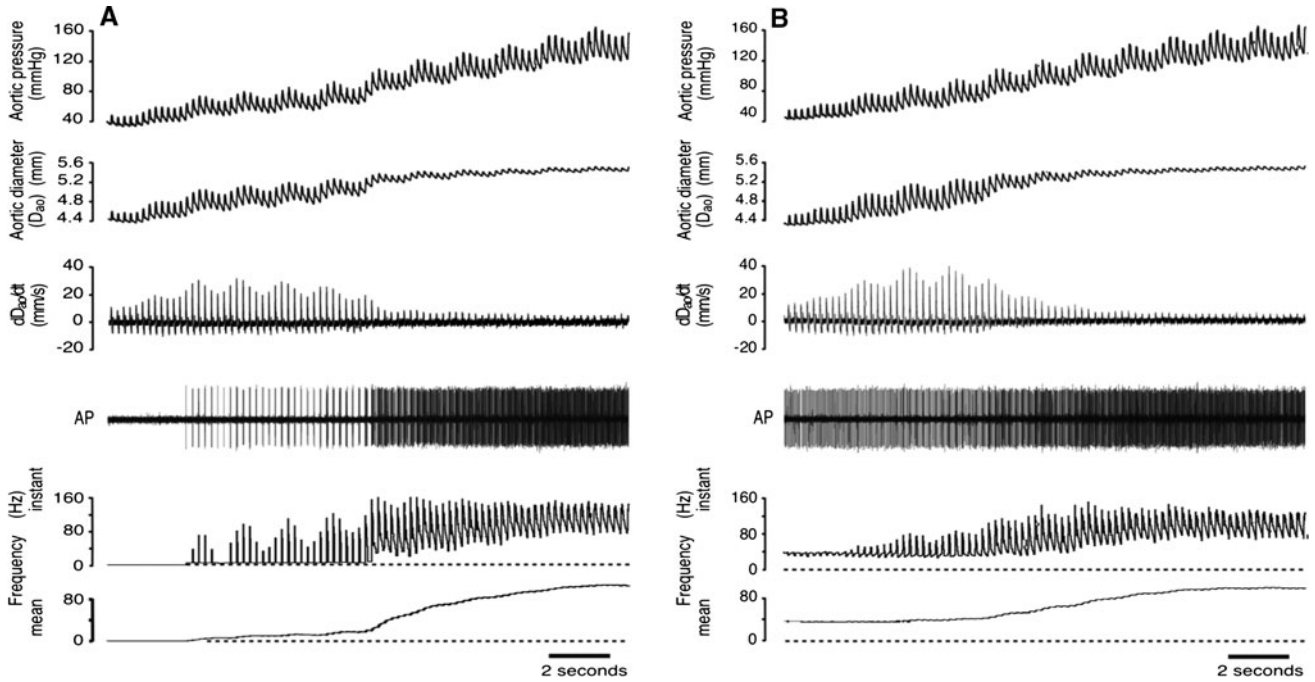

Fig. 4 **a** Record from a type A baroreceptor. The fibre is silent below P_{th}, then firing commences in systole. At higher pressures the aorta becomes stiffer such that pulse-linked fluctuations in diameter and its rate of change (dD_{ao}/dt) are reduced. These changes in circumferential wall strain are accompanied by the appearance of diastolic firing. *AP* Action potentials recorded from a single baroreceptor fibre separated from the left aortic depressor nerve. **b** Record from a type B baroreceptor, from the same animal as the fibre in **a**. This fibre fired relatively steadily and continuously at ~30 Hz until P_{th} was reached (at the 10th cycle). Below P_{th}, a small reduction in firing rate occurred early in systole. At P_{th} a distinct systolic peak in firing appears, and mean firing rate increases as pressure increases further. This particular fibre fired during both systole and diastole at all pressures examined, which was not typical of a majority of fibres regardless of their type

ramp is shown in Fig. 7. As expected [11], P_{th} was higher in the descending ramp than in the ascending ramp (~10 mmHg). Significantly, the J-shape response curve of this fibre was apparent in both ascending and descending ramps. In the descending ramp the fibre was silent for several cycles when switching from systolic to diastolic firing, indicating that this feature as well as P_{th} is sensitive to the direction of the pressure ramp.

Discussion

As far we are aware, this is the first systematic exploration and quantification of the behaviour of aortic baroreceptors at low APs. While the presence of activity in aortic baroreceptors at low pressures has been reported previously [2, 3, 11], there is no report that has quantified or explained this behaviour at low pressure. We have now demonstrated that approximately one-third of the aortic baroreceptors in the rabbit have a non-monotonic J-shaped response curve. In addition we found that 40% of all fibres were not silent at subthreshold pressures (termed autoactive fibres by Munch [3]), and these included >30% of all fibres possessing a sigmoidal response curve. When we pooled the response curves of all fibres sampled, the result resembled a multifibre curve with a distinct J-shape and substantial firing at low APs (Fig. 3b). The behaviour of the various fibre types at pressures above P_{th} was quite similar (Table 1). This suggests that a basis for the differences in their behaviour below P_{th} may be attributable to their location within the barosensory region innervated by the left ADN.

Others have reported the presence of baroreceptor activity at subthreshold pressures. In a study on the in situ preparation of the rabbit aortic arch, Angell James [2] reported that 6 of 26 single fibres from the left ADN showed constant activity over a range of 20–40 mmHg below P_{th}, and as pressure rose activity 'even diminished' before P_{th} was reached. In the same study, the importance of longitudinal strain and the tethering effect of the arteries and aorta on the discharge of aortic baroreceptors was noted. When recordings were made on in vitro preparations of the aortic arch, only 1 fibre out 31 fired at pressures below P_{th}. All of these data were obtained using a non-pulsatile pressure, so any significance of a change in strain during a pressure pulse could not have been detected. Our records (Figs. 4b, 5, 6, 7) show that the majority of firing at subthreshold pressures in type C and D fibres (J-shaped response curves) occurs during diastole. Indeed, the rising phase of systole appears to turn off firing, a reverse of the

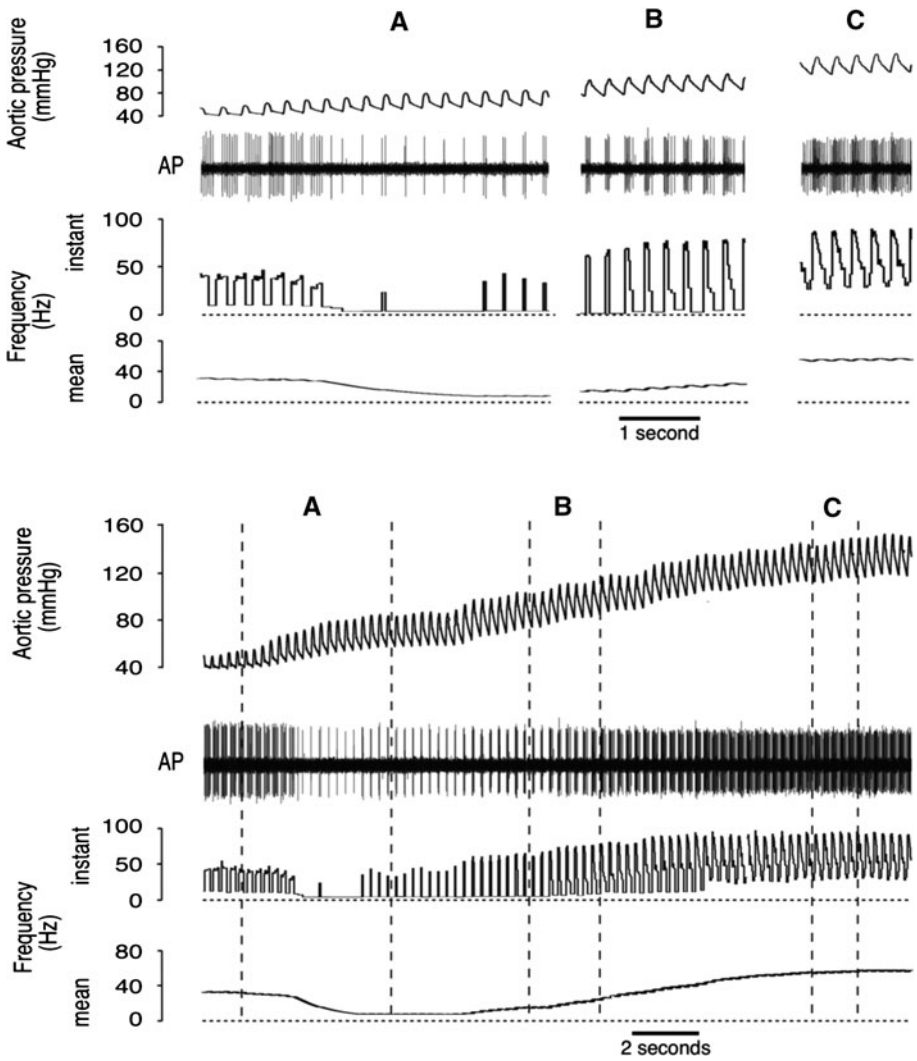

Fig. 5 Response from a type D baroreceptor. At lower pressures, these receptors usually fired during diastole. At the nadir, this fibre fired a single action potential (~4 Hz) early in systole; the mean firing rate of type D fibres at the nadir was 22 ± 16 Hz. The main point of difference in the behaviour of type D and type C fibres (not illustrated) is that type C fibres were silent at the nadir (see Table 1)

situation that occurs once P_{th} is reached. Likewise, type B fibres that fired at a steady mean frequency at pressures below P_{th} usually demonstrated a small reduction in instantaneous firing rate at the onset of the pressure pulse. Thus it appears that lower pressures may increase strain at particular locations within the barosensory area and that this strain can be temporarily relieved by the rise in pressure in early systole.

The discrete diastolic firing pattern seen in type C and D fibres occurs at values of AP where the aorta is above its unstressed volume (e.g. ~60/40 mmHg, see examples in Figs. 6, 7). It is difficult to see how falling pressure during diastole could generate an increase in circumferential strain and load baroreceptor endings within the wall of a stressed vessel. On the other hand, this baroreceptor firing pattern may be explained by the anatomy of the outer curvature of the aortic arch. Several major arterial vessels arise from the outer curvature of the arch, and baroreceptors with afferents located in both the right and left ADN are located at the origin of these arterial vessels. A reduction in pressure may increase longitudinal strain at these locations, and this strain may then be temporarily relieved by the rise in pressure in systole. Feng and colleagues [14] have examined these ideas in a theoretical and electrophysiological investigation of the axial (longitudinal) and circumferential strain in the rat aortic arch. They found that the relationship between axial strain and AP displayed a U-shape, with its minimum in the region of 70–100 mmHg. When pressure was reduced below this minimum, axial strain increased. We propose that the mechanical behaviour of the aortic arch and the response of the baroreceptors occur as follows: at lower pressures the outer curvature of the aorta will move inwards, but this movement will be opposed by the subclavian and brachiocephalic arteries that are anchored to and tether the outer curvature of the aortic arch. Baroreceptors close to the origin of the two large arteries would be subjected to increasing axial strain when pressure fell during diastole, while the rising systolic pulse

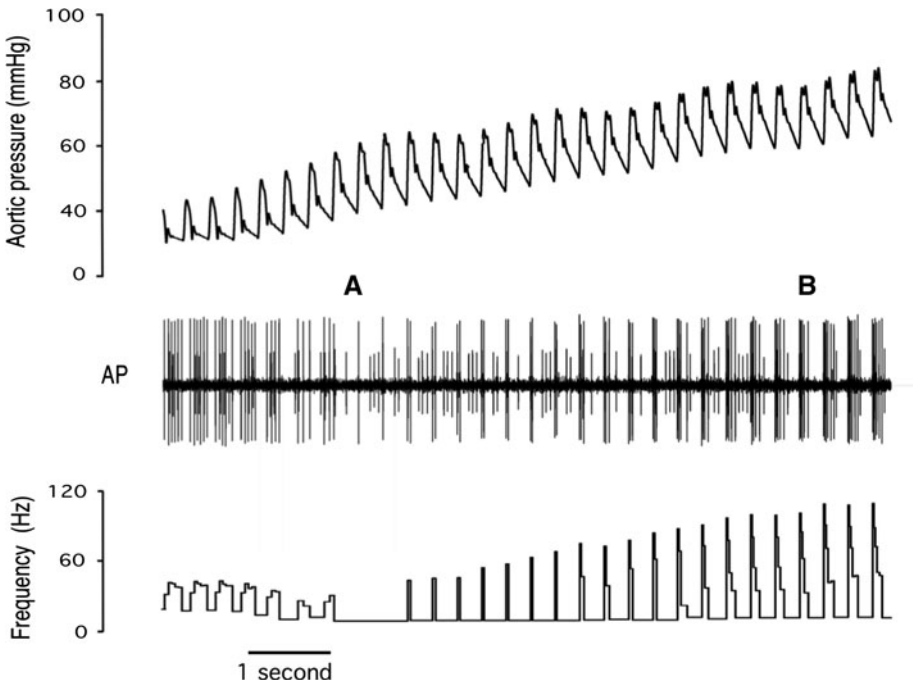

Fig. 6 Record of two type D baroreceptors. The frequency of the larger unit is shown in the *bottom trace*. At low pressures (*left* of *A*) both receptors fired during diastole. At *A*, the larger unit began firing during systole, while the smaller unit continued to fire during diastole. P_{th} for the larger unit is the pressure at *A*, while P_{th} for the smaller unit is the pressure at *B*. From their respective P_{th} values each fibre showed an increase in firing rate with increasing pressure. The mean discharge for the larger unit was identical at the lowest and highest pressures shown in this figure (six action potentials per cycle)

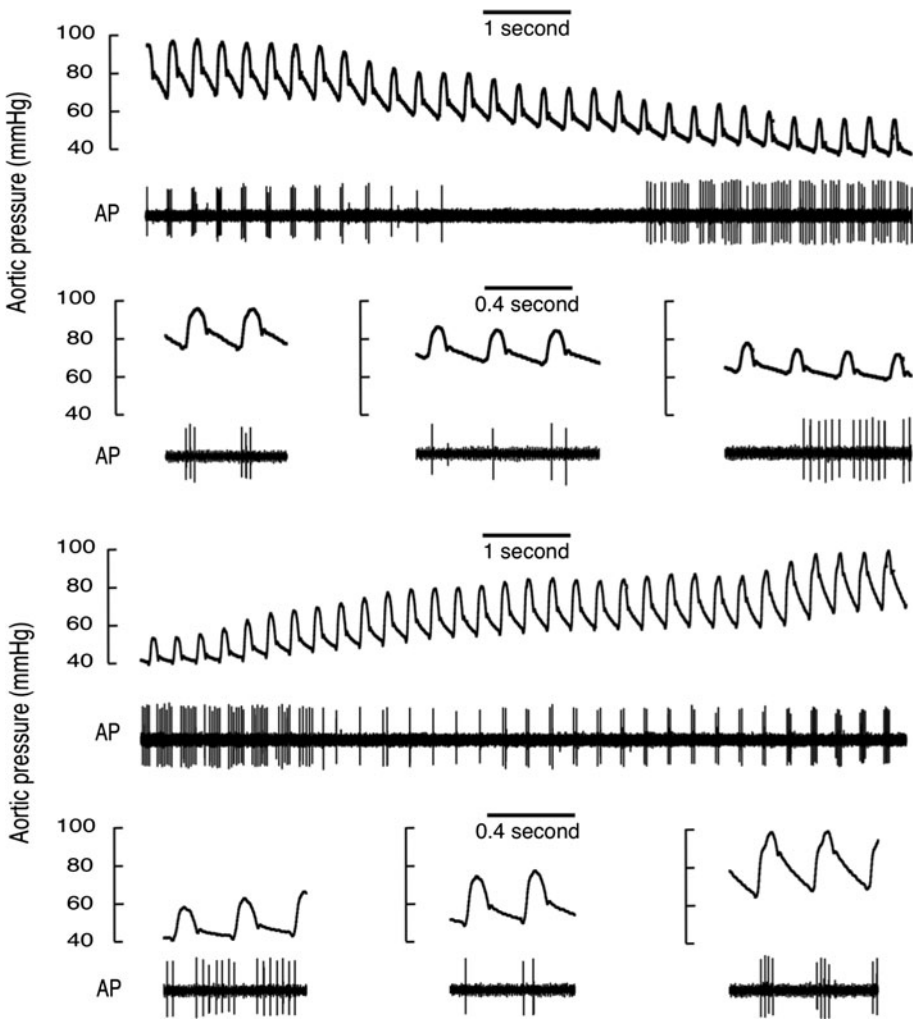

Fig. 7 Responses of a type D baroreceptor to ramps of decreasing and increasing aortic pressure. The ramps encompass baseline control and lower pressures and were obtained by gradual inflation followed by gradual deflation of a cuff around the inferior vena cava. At higher pressures in both ramps firing occurs in systole, while at lower pressures it occurs during diastole. In comparison to responses to increasing pressure, with falling pressure the baroreceptor activity tended to be lower at any particular pressure and became silent when switching between the two firing modes. All our measurements and classifications in this paper were made on ramps of increasing pressure, thus we categorised this fibre as type D rather than type C

would relieve the strain. The two baroreceptor fibres illustrated in Fig. 6 altered their firing patterns at quite different pressures. On a ramp of rising pressure, a switch from diastolic firing to systolic firing in the fibre with the larger amplitude signal occurred (at A) at a pressure ~15 mmHg lower than for the fibre with the smaller signal (switch at B). Differences in the AP at which switching occurs may be explained by differences in location of the baroreceptor endings and the potential influence of tethering in their localities.

In our study we did not identify the anatomical locations of the baroreceptor terminals associated with type C and D fibres. This would have required substantial dissection in the region of the aortic arch. As discussed below, we intentionally avoided disturbing the aortic arch in order to observe responses that were as close to natural as possible. It may be possible to identify the location of type C and D receptors using tactile stimuli [15, 16] in a preparation that has undergone further dissection but which leaves the aortic arch and the subclavian and brachiocephalic arteries relatively undisturbed.

We would expect to find a similar relationship between the distribution of wall strain and pressure in the aortic arch of other mammals, including humans. Pelletier et al. [11] described the response curves of carotid and aortic receptors in dogs to pulsatile pressure ramps and presented the response curves for four individual aortic baroreceptors (their Fig. 8). Two of the curves had a distinct J-shape, but this is not discussed in their paper. Similar responses have been recorded from baroreceptors located in other barosensory regions. Angell James [2] found that 2 of 10 baroreceptor fibres from the brachiocephalic region of the rabbit fired regularly at pressures below P_{th}.

An important feature of the present study is that the data were obtained under conditions where the aortic arch was exposed to flowing blood and pulsatile pressure fluctuations that were essentially natural. While these conditions meant that there was some variation in the pulsatile pressure pulse between preparations and during a pressure ramp procedure, the collected data will resemble signals that would occur under normal auto-perfused conditions. These conditions contrast with those of many published studies in which unnatural conditions involving pulse-free ramps, no-flow preparations, or physiological solutions replacing blood provide very reliable experimental protocols and analysis, but yield data from which extrapolation to in vivo behaviour is considerably more difficult.

We have argued that the non-monotonic response curve obtained from aortic baroreceptors possessing type C and D response curves is a consequence of the anatomy of the outer curvature of the aorta arch and associated arterial branches. The behaviour of these baroreceptors at low arterial pressure can be considered a default of the anatomical distribution of these receptors rather than as serving a particular function. It seems unlikely that pressures below P_{th} are encountered in the normal life of a rabbit. However in the event that pressure should fall below P_{th}, for example as a result of a severe haemorrhage, an increase in activity from these baroreceptors may inhibit sympathetic activity and lead to an undesirable decompensation of the haemorrhagic response. This possibility is supported by observations made during collection of data to construct baroreflex response curves (relating heart rate or sympathetic nerve activity to MAP). When MAP was reduced below the P_{th} seen in the present study by inflation of a cuff around the IVC, the raw data for heart rate [17, 18] or renal sympathetic nerve activity [17, 19] displayed a biphasic response that matched the response we predict. A majority of baroreflex studies present curves that have been fitted by mathematical expressions which do not allow for, and cannot expose, a biphasic response at subthreshold values for MAP (for an example see Fig. 1 in [19]). While the appearance of a biphasic reflex response at low pressure is congruent with the behaviour of aortic baroreceptor activity, it does not demonstrate causality.

Summary

At arterial pressures below the P_{th} of sensitivity of aortic baroreceptors to increasing pressure, a subset of baroreceptors are active. This activity occurs primarily during diastole, and its frequency is often greater than the frequency at P_{th}. The activity/pressure curve for these fibres takes on a J-shape, and the same relationship between activity and pressure is evident in whole nerve multifibre recordings. The behaviour of these baroreceptors at low pressure may be attributable to the longitudinal/axial strain in their vicinity, consequent to tethering of the outer curvature of the aorta by the subclavian and brachiocephalic arteries. It needs to be established whether the behaviour of this subset of baroreceptors at low pressures produces unusual baroreflex regulation of the circulation.

Acknowledgments This work was supported by the New Zealand Heart Foundation and the University of Otago.

References

1. Landgren S (1952) On the excitation mechanism of the carotid baroreceptors. Acta Physiol Scand 26:1–34
2. Angell James JE (1973) Characteristics of single aortic and right subclavian baroreceptor fiber activity in rabbits with chronic renal hypertension. Circ Res 32:149–161
3. Munch PA (1992) Discharge characteristics and rapid resetting of autoactive aortic baroreceptors in rats. J Physiol 458:501–517
4. Arndt JO, Dörrenhaus A, Wiecken H (1975) The aortic arch baroreceptor responses to static and dynamic stretches in an

isolated aorta-depressor nerve preparation of cats in vitro. J Physiol 252:59–78
5. Coleridge HM, Coleridge JC, Kaufman MP, Dangel A (1981) Operational sensitivity and acute resetting of aortic baroreceptors in dogs. Circ Res 48:676–684
6. Krieger EM (1987) Aortic diastolic caliber changes as a determinant for complete aortic baroreceptor resetting. Fed Proc 46:41–45
7. Xavier-Neto J, Moreira ED, Krieger EM (1996) Viscoelastic mechanisms of aortic baroreceptor resetting to hypotension and to hypertension. Am J Physiol Heart Circ Physiol 271:H1407–H1415
8. Thorén P, Munch PA, Brown AM (1999) Mechanisms for activation of aortic baroreceptor C-fibres in rabbits and rats. Acta Physiol Scand 166:167–174
9. Thorén P, Jones JV (1977) Characteristics of aortic baroreceptor C-fibres in the rabbit. Acta Physiol Scand 99:448–456
10. Yao T, Thorén P (1983) Characteristics of brachiocephalic and carotid sinus baroreceptors with non-medullated afferents in rabbit. Acta Physiol Scand 117:1–8
11. Pelletier CL, Clement DL, Shepherd JT (1972) Comparison of afferent activity of canine aortic and sinus nerves. Circ Res 31:557–568
12. Coleridge HM, Coleridge JCG, Schultz HD (1987) Characteristics of C fibre baroreceptors in the carotid sinus of dogs. J Physiol 394:291–313
13. Barrett CJ, Bolter CP (2006) The influence of heart rate on baroreceptor fibre activity in the carotid sinus and aortic depressor nerves of the rabbit. Exp Physiol 91:845–852
14. Feng B, Li B, Nauman EA, Schild JH (2007) Theoretical and electrophysiological evidence for axial loading about aortic baroreceptor nerve terminals in rats. Am J Physiol Heart Physiol 293:H3659–H3672
15. Armour JA (1973) Physiological behaviour of thoracic cardiovascular receptors. Am J Physiol 225:177–185
16. Coleridge HM, Coleridge JC, Dangel A, Kidd C, Luck JC, Sleight P (1973) Impulses in slowly conducting vagal fibers from afferent endings in the veins, atria and arteries of dogs and cats. Circ Res 33:87–97
17. Nishida Y, Ryan KL, Bishop VS (1995) Angiotensin II modulates arterial baroreflex function via a central α1-adrenoceptor mechanism in rabbits. Am J Physiol Regul Integr Comp Physiol 269:R1009–R1016
18. Brooks VL, Clow KA, O'Hagan KP (2002) Pregnancy and acute baroreflex resetting in conscious rabbits. Am J Physiol Regul Integr Comp Physiol 283:R429–R440
19. O'Hagan KP, Casey SM (1998) Arterial baroreflex during pregnancy and renal sympathetic nerve activity during parturition in rabbits. Am J Physiol Heart Circ Physiol 274:H1635–H1642